

See discussions, stats, and author profiles for this publication at: <https://www.researchgate.net/publication/231704734>

Mixed Mode Thiol–Acrylate Photopolymerizations for the Synthesis of PEG –Peptide Hydrogels

ARTICLE *in* MACROMOLECULES · JULY 2008

Impact Factor: 5.8 · DOI: 10.1021/ma800621h

CITATIONS

90

READS

225

2 AUTHORS, INCLUDING:



Kristi Anseth

University of Colorado Boulder

356 PUBLICATIONS 20,379 CITATIONS

SEE PROFILE

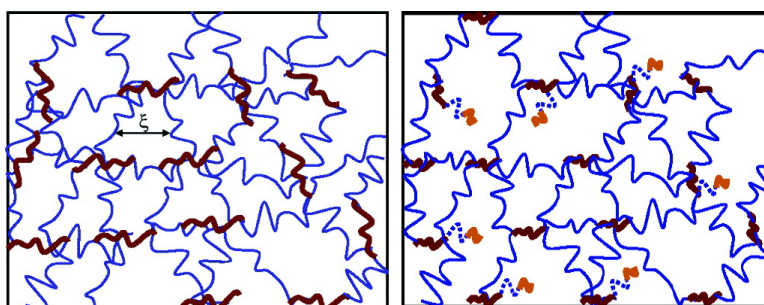
Article

Mixed Mode Thiol#Acrylate Photopolymerizations for the Synthesis of PEG#Peptide Hydrogels

Chelsea N. Salinas, and Kristi S. Anseth

Macromolecules, **2008**, 41 (16), 6019-6026 • DOI: 10.1021/ma800621h • Publication Date (Web): 23 July 2008

Downloaded from <http://pubs.acs.org> on April 13, 2009



More About This Article

Additional resources and features associated with this article are available within the HTML version:

- Supporting Information
- Links to the 1 articles that cite this article, as of the time of this article download
- Access to high resolution figures
- Links to articles and content related to this article
- Copyright permission to reproduce figures and/or text from this article

[View the Full Text HTML](#)



ACS Publications
High quality. High impact.

Macromolecules is published by the American Chemical Society, 1155 Sixteenth Street N.W., Washington, DC 20036

Mixed Mode Thiol–Acrylate Photopolymerizations for the Synthesis of PEG–Peptide Hydrogels

Chelsea N. Salinas[†] and Kristi S. Anseth^{*,†,‡}

Department of Chemical and Biological Engineering and Howard Hughes Medical Institute, University of Colorado, Boulder, Colorado 80309

Received March 19, 2008; Revised Manuscript Received June 19, 2008

ABSTRACT: Thiol–acrylate mixed mode photopolymerizations provide an easy, robust, cost-efficient, and cytocompatible reaction scheme for the incorporation of cysteine-containing peptide sequences into PEG hydrogels. With an acrylate:cysteine ratio of 4:1, ~95% of the peptide is incorporated after 10 min of reaction with ~5 mW/cm² of 365 nm light. Specifically, thiol monomers, with thiol-presenting peptide groups in the form of CGGGGG, CRGGGG, CWGGGG, CDGGGG, CSGGGG, and CGGGGC, copolymerized with PEG4600 diacrylate were characterized. The chain transfer constant of acrylates to thiols was determined to range from 1.5 to 2, depending on the amino acid sequence. Complete conversion of the functional groups occurred after ~40 s for all systems, excluding the tryptophan-containing peptide sequence which had a retarded polymerization, taking ~60 s. The cross-linking densities of the final gels ranged from 1.5×10^{-2} to 2.0×10^{-2} mol/L when 10 mM of peptide was reacted with 40 mM of acrylate groups. Efficient incorporation of high amounts of peptide functionalities with this polymerization method provides a facile technique for the covalent incorporation of cell-specific peptides important for directing cellular function in a gel environment and the purposes of 3D cell culture, which are critical in applications such as tissue engineering.

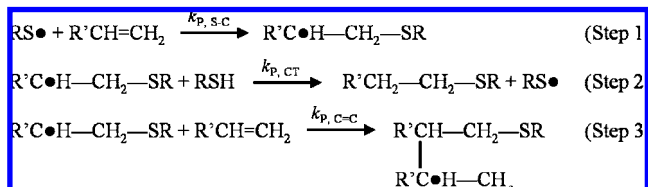
1. Introduction

The use of peptide-modified materials for the purposes of tissue engineering has grown over the past decade and is now a widely studied area of interest. Synthetic and inert material systems, such as poly(ethylene glycol) (PEG) hydrogels, provide little in the way of directed cues for entrapped cells, causing them to alter their cellular functions and production of essential extracellular matrix (ECM) components and often lead to apoptosis.^{1,2} Therefore, to specifically direct cell survival and cell function, ECM components selected from the tissues being recreated are often necessary in this process. For the application of tissue engineering, tailoring of the gel chemistry is often essential.³ One approach is to incorporate peptide sequences that initiate cell-binding and cell-signaling events, mimicking the native signaling of cells.^{4,5} While incorporation of peptide sequences into PEG gels has been used to direct cellular function, new directions in polymerization mechanisms have allowed advances into the modification of PEG materials over the past decade.

Modification of PEG gels to include specific peptide sequences can be achieved through many different methods, including covalently linking peptides to a monoacrylated PEG monomer through an *N*-hydroxysuccinimidyl group.⁶ This method presents a means to recover high yields of PEGylated peptides, and the approach is similar to classical methods for coupling proteins to PEG.^{7,8} While use of asymmetrically modified PEGs has been extensively studied over the past decade, this method only allows for synthesis of tethered peptides and requires the use of expensive reagents. Alternatively, cysteine-containing peptide sequences have been reacted into hydrogels through Michael-type addition.^{5,9,10} The mechanism for Michael-type addition is base-catalyzed, which causes a step growth reaction between -ene functional groups, those most often studied being acrylates,¹¹ maleimides,¹² acrylamides,¹³ and sulfones.¹⁴ This method allows facile incorporation

of cysteine-containing peptides with appropriately functionalized PEG macromers and proceeds via a stepwise growth mechanism. However, this reaction requires a careful balance of the stoichiometry of the functional groups, and this ultimately affects the final network structure and properties. Further, stepwise growth reactions have delayed gel points compared to chain polymerizations, which can be beneficial in relieving polymerization-induced stresses but can be complicated for in situ forming biomaterials or cell encapsulate protocols. While extensive research has been conducted involving this reaction scheme to shorten the gelation and polymerization time through delicate monitoring of the system pH, alternative approaches that are not limited by stoichiometric ratios, polymerization time, or pH would provide specific benefits in biomaterial applications.

This research uses cysteine-functionalized peptide sequences in combination with multifunctional PEG–acrylates but employs a *photoinitiated* mixed-mode polymerization mechanism. Photoinitiated thiol–ene and thiol–acrylate mechanisms have been studied extensively with the use of numerous low-molecular-weight, aliphatic, tetrathiols in combination with vinyl ethers, allyl ethers, or acrylate monomers.^{15–17} Briefly, the reaction mechanism consists of two competing reactions; that of the acrylate homopolymerization and the thiol–acrylate step growth reaction,¹⁶ as outlined below. Here the kinetic constants are as



follows: $k_{\text{p},\text{S-C}}$ is the chain transfer constant for the intermediate formed through the stepwise reaction of a thiyl radical with a vinyl group, $k_{\text{p},\text{CT}}$ is the chain transfer constant for the reaction between the carbon radical intermediate with a thiol, and $k_{\text{p},\text{C-C}}$ is the propagation kinetic constant for the homopolymerization of a carbon-based radical intermediate with a vinyl group. The polymerization is initiated photochemically and proceeds through

* To whom correspondence should be addressed: phone (303) 492-3147, fax (303) 492-4341.

[†] Department of Chemical and Biological Engineering.

[‡] Howard Hughes Medical Institute.

Table 1. $k_{P,C=C}/k_{CT}$, pK_a , and % Incorporated Values for Peptide Sequences with Variations in the Amino Acid in the Primary Position

peptide sequence	CGGGGG	CRGGGG	CWGGGG	CDGGGG	CSGGGG	CGGGGC
$k_{P,C=C}/k_{CT}$	1.5	1.2	2.1	1.6	1.3	1.1
pK_a	8.4 ± 0.8	8.2 ± 0.9	8.8 ± 0.8	8.5 ± 0.7	8.3 ± 0.6	8.3 ± 0.8
% incorporated	94 ± 1	95 ± 2	87 ± 3	92 ± 1	93 ± 1	97 ± 2

the above-outlined simultaneous stepwise growth (i.e., thiol–acrylate reaction, steps 1 and 2) and chain polymerization (i.e., acrylate homopolymerization, step 3).^{15,16} Depending on the functionality of the monomers, polymer networks are readily synthesized. The competition of acrylate homopolymerization with the thiol–acrylate step growth network formation leads to very different reaction kinetics and final network structures than obtained with purely step growth polymerization (i.e., thiol–ene or Michael-type addition, of those mentioned here)^{9,16,18} or chain polymerizations of multivinyl monomers.^{19–21}

Previous researchers have determined that the acrylate chain growth occurs at a faster rate than that of the step growth reaction, leading to a chain transfer constant of $k_{P,C=C}/k_{CT} = 1.5$, as derived by fitting functional group conversion profiles to the following equation:¹⁵

$$\frac{d[C=C]}{d[SH]} = 1 + \left(\frac{k_{P,C=C}}{k_{CT}} \right) \frac{[C=C]}{[SH]} \quad (1)$$

Here, $[C=C]$ represents the concentration of acrylate functional groups, where $[SH]$ represents the concentration of thiol functional groups in the reaction. These studies of mixed mode thiol–acrylate reactions have been used to provide evidence in support of kinetic models,^{15,16,22} mechanistic schemes,^{17,23} and reaction rates¹⁶ of these unique systems. However, little evidence has shown how the thiol–acrylate reaction scheme can translate to a system where peptides are used as the thiol-containing monomer.^{16,23} Peptides, different from their aliphatic thiol counterparts, can vary in amino acid sequence, charge, size, and reactivity of the side groups. The length and sequence of a peptide can result in disulfide bond formation or lead to the formation of secondary structure (i.e., folds) in the molecule. The reactivity of the thiol, found on the cysteine group, is likely affected by amino acids in the primary position of the sequence that is directly next to the cysteine.^{9,18,24} The objective of this work was to exploit the thiol–acrylate polymerization as a means to design new PEG–peptide gel chemistries that promote specific cell interactions and functions. It is noted that peptide modification of PEG monomers via the thiol–acrylate mixed mode reaction may vary from previously studied thiol–acrylate reaction schemes based on aliphatic, tetrafunctional thiols, acrylates, vinyl ethers, and allyl ethers. In this work, we aimed to characterize and understand potential differences when cysteine functionalities are used as the thiol-presenting monomer in this reaction mechanism. For biomaterial applications, the extent of reaction, rate of polymerization, and final network structure all have important implications when employing this reaction mechanism to create peptide-functionalized gels.

2. Results and Discussion

Multifunctional thiol–acrylate photopolymerization reactions and the resulting polymer network structures were analyzed. The kinetic chain transfer constants and conversion of the functional groups as well as the cross-linking density, elastic modulus, and pK_a values of the reacting thiol group were measured for the copolymerization of the following peptides with PEG4600DA: CGGGGG, CRGGGG, CWGGGG, CDGGGG, CSGGGG, and CGGGGC. All reactions mixtures were conducted at thiol:acrylate functional group ratios of 1:4. A ratio of 1:4 thiols:acrylates was selected as it provides a concentration range that is biologically relevant for many peptides. Information

regarding the relative conversion of the functional groups and final network formation was sought to understand the overall peptide incorporation into PEG networks and characterize how this reaction mechanism influences the final network structure and material properties.

2.1. Functional Group Conversion. Near-FTIR measurements, to measure acrylate conversion, alongside Ellman's assay, to measure thiol conversion, were used to determine the conversion profiles of these functionalities in a thiol–acrylate mixed mode photopolymerization scheme of CGGGGG, CRGGGG, CWGGGG, CDGGGG, CSGGGG, or CGGGGC with PEG4600DA. Further free amine measurements were collected for each system prior to polymerization and from the soluble fraction after polymerization to determine the amount of peptide incorporated. Each system contained 10 mM thiol functional groups compared to 40 mM acrylate functional groups. Using eq 1, the chain transfer constant for each of the PEG–peptide systems was calculated as well as the amount of peptide incorporated and is summarized in Table 1. Previously determined chain transfer constants for this type of reaction using low-molecular-weight, aliphatic thiols with acrylates was found to be ~ 1.5 . When peptide sequences containing a thiol-presenting cysteine amino acid is used as the thiol monomer, it was found that deviations from the $k_{P,C=C}/k_{CT} = 1.5$ exist, dependent upon the amino acid in the primary position next to the cysteine. PEG–peptide systems containing a glycine or aspartic acid in the primary position do not alter the kinetics considerably, with measured chain transfer constants of 1.5 or 1.6 and peptide incorporation rates of $\sim 93\%$. When an arginine or serine is in the primary position or when the peptide sequence has two cysteines on either end of the peptide, the $k_{P,C=C}/k_{CT}$ decreases to less than 1.5 (i.e., 1.1–1.3). Similarly, the percent of peptide incorporated reached $\sim 97\%$, meaning that in these systems the thiol and acrylate functional groups are more reactive than that seen with aliphatic thiols. These variations in the kinetics are most likely attributed to the charged groups or the hydrogen acceptors found on the side chains of arginine, serine, or cysteine, thereby increasing the likelihood of cysteine radicalization and reaction. Finally, if a tryptophan exists in the primary position, the $k_{P,C=C}/k_{CT}$ increases to 2.1, and the percent of peptide incorporated decreased to $87 \pm 3\%$. Therefore, in the tryptophan system, a slightly larger amount of thiol is left unreacted as compared to the previously mentioned PEG–peptide systems. The tryptophan amino acid sequence possesses a large side chain, which can sterically interfere with radical initiation or covalent attachment.

Model predictions of the thiol:acrylate conversion, as derived in eq 1, were plotted against experimental data, as seen in Figure 2A,B. The variations in $k_{P,C=C}/k_{CT}$ for each system correspond well to the experimentally determined conversion of these species, lending to the fact that alterations in the $k_{P,C=C}/k_{CT}$ can affect the ultimate functional group conversion for these peptide-containing systems. The $k_{P,C=C}/k_{CT}$ values were seen to vary from the 1.5 value, as determined with aliphatic thiols, based upon the amino acid found in the primary position. By changing the charge or side groups of the primary amino acid, the conversion and, therefore, reactivity of the thiol presenting cysteine group were altered. Further investigation was completed to verify that the changes in conversion and chain transfer constants were indeed a result of amino acid composition and position.

2.2. Alteration in Thiol Reactivity with Variations in Peptide Sequence Composition. To better understand variations in the reactivity of the peptide thiols as a function of these sequences, an investigation into the pK_a changes that occur to the cysteine as a function of differing amino acids in the primary position was conducted. These pK_a values were determined experimentally as described previously by Lutolf.¹⁸ Briefly, the absorbance by the thiol group was measured for each peptide sequence at varying pHs. pK_a values were determined from the following equations, where A_{\max} is the absorbance of the thiol group at the highest pH level, A_i is the absorbance at that specific pH level, and C_{thiol} is the concentration of thiol in solution:¹⁸

$$-\log([SH]_i/[S^-]_i) = pH_i - pK_a \quad (2)$$

and

$$[SH]_i/[S^-]_i = (C_{\text{thiol}} - [S^-]_i)/[S^-]_i = (A_{\max} - A_i)/A_i \quad (3)$$

From eq 3, the plot of $-\log[(A_{\max} - A_i)/A_i]$ vs pH yields a graphical line, whereby the intercept of the line with the x -axis provides the pK_a value for that specific peptide sequence. These pK_a values are summarized in Table 1, and an example of pK_a determination is depicted in Figure 3. As seen previously by Lutolf,¹⁸ when examining the reactivity of thiol-containing peptide sequences for Michael-type addition, the positively charged amino acids in the primary position lowers cysteine's pK_a , while negatively charged amino acids increases the pK_a . A decrease in pK_a values was observed to create more thiol radical species, thereby increasing the reaction rate of the peptide sequences, and vice versa. Cysteine typically has a pK_a value between 8.4 and 8.5. The results for this study indicate that the

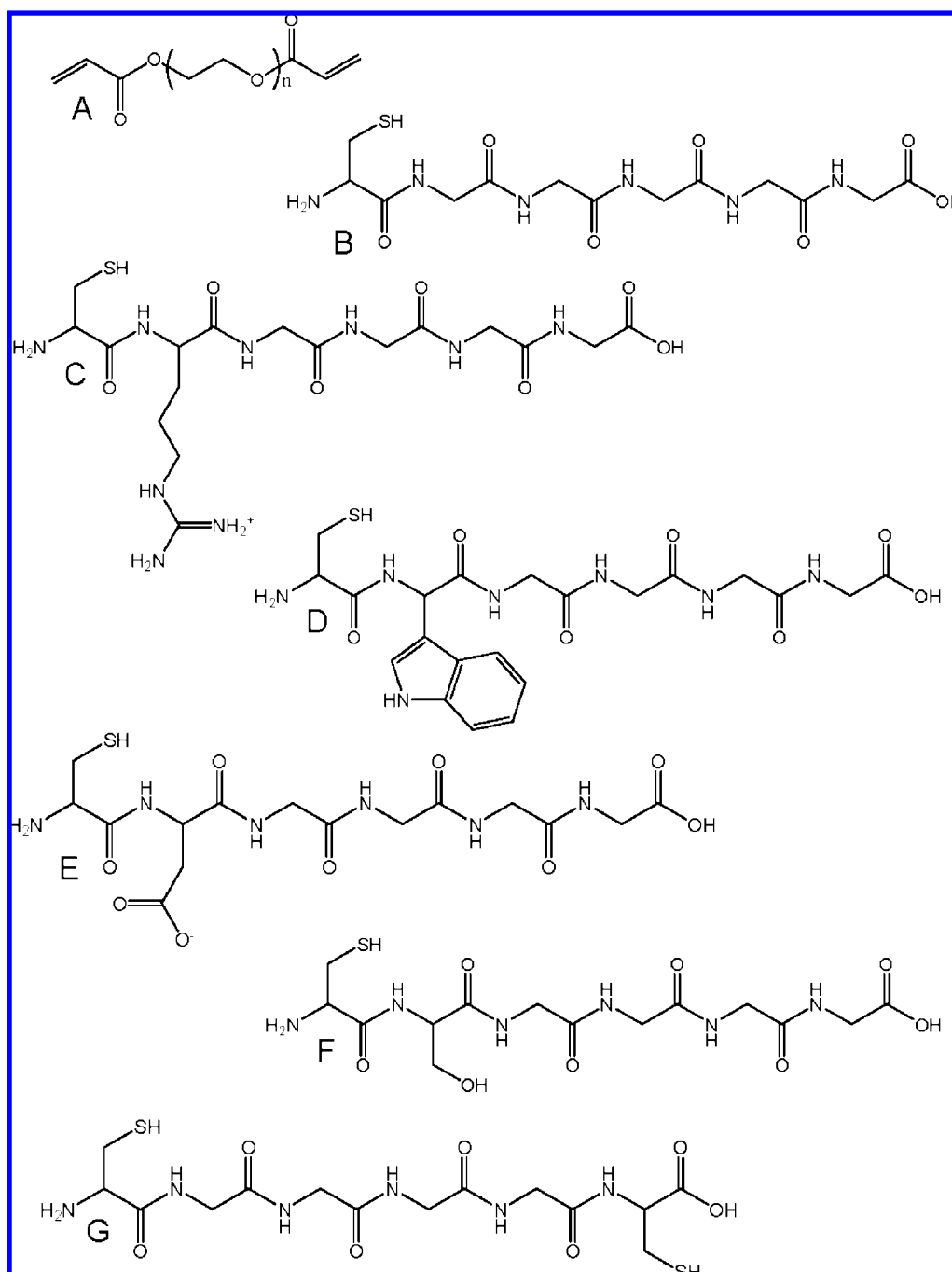


Figure 1. Chemical structures for components used in this study: (A) PEGDA, (B) CGGGGG, (C) CRGGGG, (D) CWGGGG, (E) CDGGGG, (F) CSGGGG, and (G) CGGGGC.

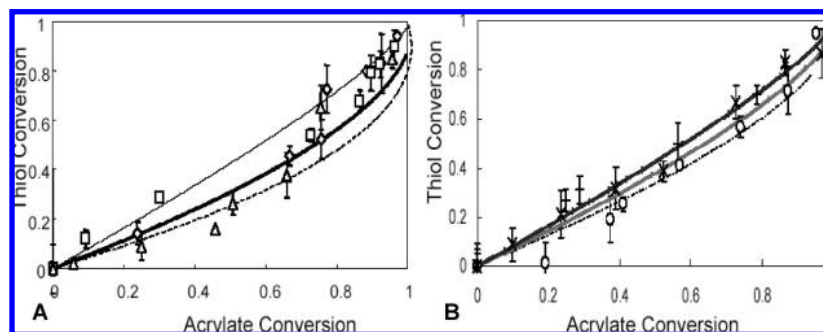


Figure 2. Comparison of experimental data to model predictions using the $k_{p,C=C}/k_{CT}$ values determined for each peptide sequence. All peptides are reacted at 10 mM with a 40 mM, 10 wt % PEG(4600) DA and are reported as follows: (A) CGGGGG (◇), CRGGGG (□), and CWGGGG (△). (B) CDGGGG (○), CSGGGG (×), and CGGGGC (+).

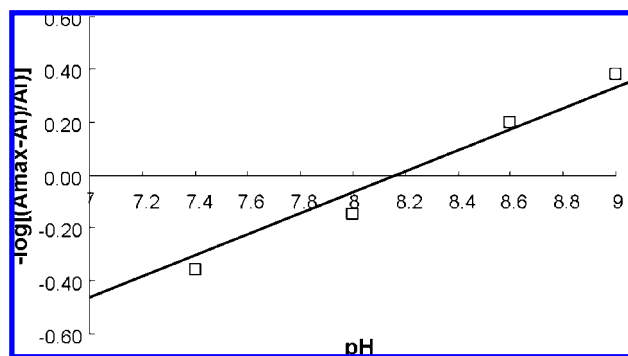


Figure 3. Depiction of pK_a determination for the PEG–CRGGGG system. Peptide absorbance was measured at a variety of pH values and plotted as based upon the log of the maximum and initial absorbance values. A line was drawn through the values and the intersection of the x-axis provided the pK_a value.

positively charged arginine group decreases the pK_a to 8.2 ± 0.3 , and the same decrease in pK_a was also seen for the serine and dicysteine group. When glycine or aspartic acid is present in the primary position, there was a minimal effect on the pK_a , indicating that these peptide sequences may have a nominal effect on the reactivity of the thiol group. A tryptophan in the primary position greatly increased the pK_a value, thereby limiting the number of reactive thiol groups in solution and hindering the reaction process as well.

With an understanding of the change in pK_a values for the thiol-presenting cysteine amino acid, further speculation aids in explaining the cause of the pK_a and reactivity deviation. Amino acid interactions are complex and can easily alter the properties of peptide sequences and proteins. The amino acids chosen for this study were selected to cause interactions with the cysteine and therefore alter the kinetics of the thiol–acrylate mixed mode photopolymerization reaction to better understand this process. Glycine is an aliphatic amino acid, which was chosen to be more representative of previously studied low-molecular-weight, aliphatic thiols. This amino acid should have negligible effects on the chemical properties of cysteine as it is extremely inert. The arginine and aspartic acid groups are charged, and the arginine group has been shown to increase the rate of deprotonation of the thiol group, whereas the aspartic acid hinders this process.^{18,24} This explanation supports the results shown here where a decrease in pK_a corresponding to an increase in $k_{p,C=C}/k_{CT}$ for the arginine group. The opposite is observed for the aspartic acid group, although less significant.

The serine group is known to have a strong hydrogen-bonding capacity through its hydroxyl group, thereby increasing the rate of deprotonation of the thiol group and increasing the kinetics of this peptide, which corresponds to the data collected for this sequence. Tryptophan introduces an amino acid with a large

side chain, which may not only affect the kinetics of the reaction due to steric hindrance of the thiol reactive group, but the indole group is also known to hydrogen donate under some situations. If the indole hydrogen donated under the circumstances presented in this experiment, this amino acid can easily hinder the radicalization of the cysteine. Furthermore, the indole functionality absorbs strongly in the 280 nm region with minimal, if any, absorption at 365 nm, providing limited opportunity to interfere with the photoinitiator absorption of the initiating light. Therefore, the presence of the indole group and its possible hydrogen donation, along with steric hindrance effects, can significantly decrease the pK_a and limit the reactivity of the thiol group, which is supported by the data presented in Table 1. Finally, the dicysteine functional sequence contains a cysteine group on each side of the peptide composed of inert glycine groups. Although the cysteines are not directly next to one another in the sequence, the interaction of two cysteine functionalities from the sequences in solution can have deleterious effects on the reactivity of this peptide. Cysteine can form disulfide bonds, which limit the concentration of reactive thiol-presenting cysteines in solution. Although a decrease in pK_a was seen, this simply means that the cysteines are slightly more reactive than normal and could very well interact with themselves more so than with the acrylate group.

2.3. Network Structure of Thiol–Acrylate Photopolymerized PEG–Peptide Systems. For these same comonomer compositions and reaction conditions, the time to the gel point, final network formation, and real time evolution of the elastic modulus of the PEG–peptide gels were measured using real-time rheology, where the sample was photopolymerized in situ during the measurement process. This data are presented in Table 2 along with a schematic figure of the network structures of PEG–diacrylate and a PEG–peptide system (Figure 5). Rheological data provided evidence that the crossover point (i.e., an estimate of the time to reach gelation²⁵) for these systems did not vary considerably as the peptide composition was varied. Most systems gelled within ~ 40 s, with the exception of the tryptophan-containing peptide system. Just as the tryptophan-containing sequence was seen to increase the $k_{p,C=C}/k_{CT}$ value and decrease the overall polymerization rate, the gelation time was also delayed for this system to ~ 60 s. The observed delay in the crossover point implies that the presence of the tryptophan moiety is hindering the homopolymerization of the acrylate groups through either steric hindrance or decreased inherent reactivity of the thiol radical.

Rheological data also provided information regarding the total time to reach maximum functional group conversion for each system studied. Specifically, the final polymerization time was determined from the plateau of the elastic modulus. In comparing all samples studied, the pure PEG–diacrylate network was completely polymerized after ~ 100 s, while the PEG–peptide

Table 2. Material Properties for Each PEG–Peptide System Polymerized at 5 mW/cm², Including Crossover Time, G' , ρ_x , and Q

sequence	PEG	CGGGGG	CGGGGC	CRGGGG	CSGGGG	CDGGGG	CWGGGG
crossover time (s)	43 ± 3	38 ± 1	36 ± 2	39 ± 3	40 ± 1	39 ± 2	55 ± 5
elastic modulus, G' (kPa)	22 ± 5	17 ± 3	17 ± 6	17 ± 8	17 ± 5	18 ± 1	19 ± 3
cross-linking density 10 ⁻² (mol/L) ^a	2.0 ± 0.3	1.6 ± 0.3	1.5 ± 0.2	1.5 ± 0.1	1.5 ± 0.3	1.6 ± 0.1	1.7 ± 0.2
equilibrium swelling (Q)	19.2 ± 0.9	30.2 ± 1.2	31.1 ± 1.0	26.5 ± 0.3	21.5 ± 0.8	22.1 ± 0.6	24.3 ± 1.4

^a Cross-linking density calculations based upon elastic modulus at 25 °C and 90 wt % water content for all samples measured relating to a Q of 10.63.

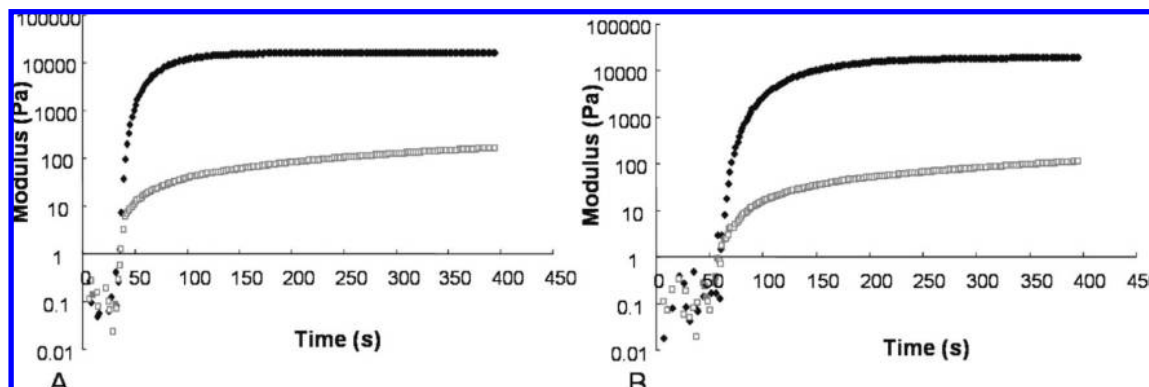


Figure 4. Rheological data for PEG–CRGGGG (A) and PEG–CWGGGG taken during a time sweep polymerized at 5 mW/cm². When the G' , elastic modulus (black line), and the G'' , storage modulus (open line) cross, this initiates the dominance of the G' throughout the remainder of polymerization. The final material properties can be obtained from this data at an equilibrium G' value. Here the R-containing peptide sequence polymerizes at a faster rate than that of the W-containing peptide sequence.

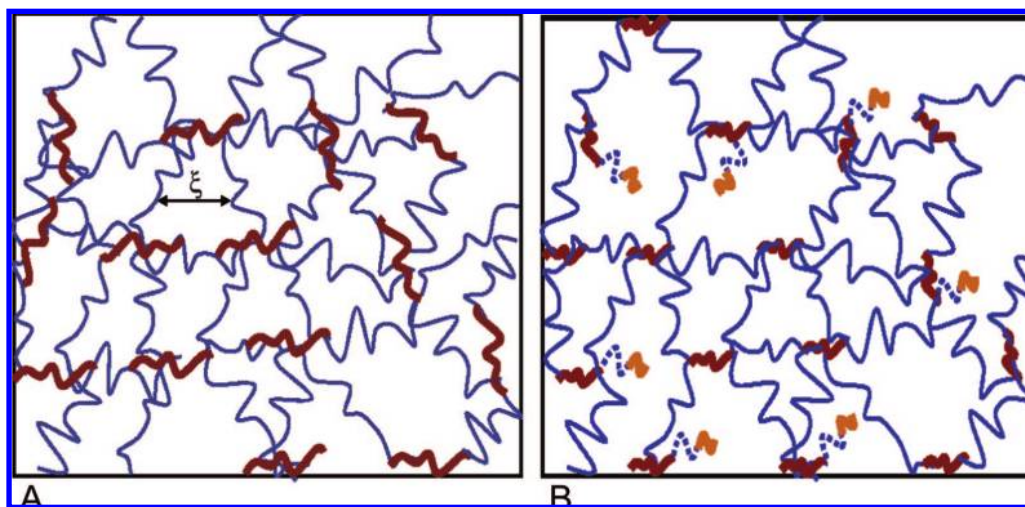


Figure 5. Schematic structure for covalently cross-linked networks composed of multifunctional macromers. Here red represents a polyacrylate kinetic chain, blue depicts the swollen PEG cross-links, and dotted blue plus orange represents a PEG–peptide chain. (A) The kinetic chains are representative of covalent bonds between PEG chains. The mesh size (ξ) depicts the physical distance between cross-links and can be correlated to the equilibrium swelling ratio (Q).³¹ (B) Schematic of the mixed-mode copolymerization process between a PEGDA and a thiol-containing peptide sequence.

systems were slightly faster, polymerizing in 90–96 s, with the exception of the tryptophan-containing system. The PEG–peptide containing tryptophan reached its maximum conversion after ~110 s. Interestingly while the time to reach the final conversion varied in these systems, the final network structures as characterized by the elastic modulus were relatively similar. As depicted in the schematic seen in Figure 4A, the PEGDA system is created via a radical chain solution polymerization of macromolecular PEG diacrylate monomers, which result in a nodal type network formation (i.e., collapsed polyacrylate kinetic chains cross-linked by extended PEG chains in an aqueous environment). When the PEGDA is copolymerized with a polyglycine sequence with a terminal cysteine group, this thiol–acrylate shortens the average kinetic chain length because of chain transfer to the thiol presenting peptide groups. These short peptides sequences are covalently bound to the polyacry-

late nodes, but the overall gel structure does not change significantly, as measured by the modulus for the ratio of thiols to acrylates used in these studies. The data presented show that pure PEGDA, polymerized via chain polymerization, has a modulus of ~23 kPa, while the PEG–glycine gel, polymerized via the mixed-mode mechanism, has a slightly lower, but not statistically different, modulus of ~17 kPa. Further, when the polyglycine was functionalized with cysteines on both ends, the final gel modulus was relatively unchanged (~17 kPa), which further supports the concept of the general network structure. This data indicates that these two peptides create similar network structures, which provides evidence that the dicysteine peptide is being incorporated in a looplike structure, within one kinetic chain, as opposed to a cross-linker between multiple kinetic chains. With the other peptide sequences studied, there was a slight decrease in modulus as compared to the PEGDA network

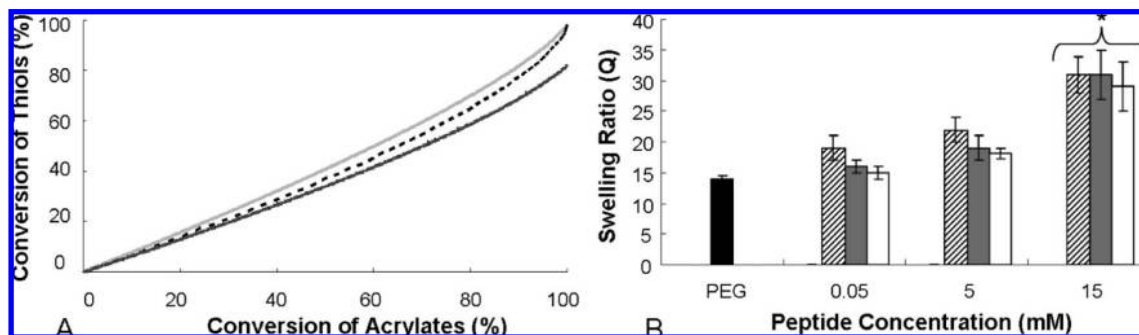


Figure 6. (A) Model predictions for the conversion of thiols and acrylates at different initial thiol concentrations. Acrylate:thiol concentrations for model predictions are as follows: 43:0.05 (gray line), 43:5 (dotted line), and 43:15 (black line). (B) Swelling ratios for different concentrations of peptides reacted with the PEG4600DA. Concentrations ranged from 0.05 to 15 mM peptide. A gel formed from the chain homopolymerization of pure PEG—diacrylate was used as a comparison. CGGGGG (dashed bars), CRGGGG (gray bars), and CWGGGG (white bars). All PEG—peptide systems polymerized at a peptide concentration of 15 mM had significantly higher swelling ratios than the lower peptide concentrations (* $p < 0.05$).

relating to more possible space within these networks due to the incorporation of tethered peptide groups; however, this data is not significant.

The cross-linking density was estimated as a function of the elastic modulus from rheological data and the water content in the samples during testing as follows:^{26–28}

$$\rho_x = \frac{G_{\text{meas}}}{RT(10.63)^{-1/3}} \quad (4)$$

Here, G_{meas} is the elastic modulus from rheological data (Pa), R is the gas constant ($\text{cm}^3 \text{ Pa}/(\text{mol K})$), T is the temperature (K), and 10.63 relates to the amount of water in the system during modulus measurements on the rheometer based upon 90 wt % water (equivalent for all samples). A summary of the experimental data, along with the calculations, is presented in Table 2. As dictated by eq 4, the cross-linking density trends are similar to that of the measured elastic modulus, whereby the cross-linking density for those samples containing peptide sequences was slightly less than that of pure PEG. Yet, statistically, differences between the cross-linking densities of all samples tested were not significant.

Finally, equilibrium swelling measurements were also investigated to better understand the effect of compositional variations (e.g., peptide charge and hydrophobicity) on the equilibrium swelling ratio (Q). For the same chemistry, one would expect the swelling ratio to follow the trends in the cross-linking density; however, with the incorporation of peptide groups into the PEG systems, the chemistry plays an important role in dictating the final water content in these systems. The results are also summarized in Table 2. Again, the monocysteine PEG—glycine network shows similar swelling when compared to the dicysteine PEG—glycine network where both have a resultant equilibrium swelling of ~ 30 . The PEG—glycine networks show the highest degree of swelling over all other PEG—peptide systems. Further, incorporation of the positively charged arginine was seen to have a higher swelling ratio than that of the charged aspartic acid group. This phenomenon is most likely related to the likelihood of arginine interacting with the more accessible negative charges on a water molecule.

While investigations were focused on the reactivity of the cysteine group as mediated by the amino acid in the primary position, further experiments were conducted to understand the effects of peptide functionality on final network properties. The commonly used amino acid RGDS was incorporated in a similar fashion at a concentration of 10 mM peptide to a 10 wt % PEG4600DA monomer (40 mM). Experiments with the RGDS peptide showed insignificant differences in the swelling ratio, with a value of 24.3 ± 0.8 as compared to that of the CRGGGG

system with a Q value of 26.5 ± 0.3 . Further, rheological data showed that the RGDS-containing gel resulted in an elastic modulus of 19 ± 5 kPa, while the PEG—CRGGGG gel had a modulus of 17 ± 8 kPa. This study provides evidence that while the functionality of a peptide sequence may have an effect on the interactions with molecules or cells, there are very few differences seen in the gel properties when the amino acid in the primary position remains the same.

To better understand the effect of the initial comonomer ratio (i.e., thiol:acrylate) on the gel structure and properties, a second study was conducted using a range of ratios of thiols:acrylates for the PEG—glycine, PEG—arginine, and PEG—tryptophan systems as compared to that of a pure PEG—acrylate gel. Systems were synthesized from a 10 wt % PEG4600DA monomer (40 mM) and reacted with 0.05, 5, and 15 mM concentrations of those peptide sequences listed above. Based on the previous kinetic characterization, model predictions are presented in Figure 6A which illustrate the rate of thiol vs acrylate conversion at these different comonomer ratios. Consistent with the polymerization mechanism, an increase in the initial thiol concentration leads to a decreased rate of consumption of the acrylate and a final conversion of acrylate that is less than 1 at the highest thiol:acrylate ratio studied. Further, the increased thiol content alters the network structure, as a result of greater chain transfer and shorter kinetic chains. This was observed by measuring the equilibrium mass swelling ratio as a function of the gel composition. In comparing the swelling ratios of the G-, R-, and W-containing peptides, all those PEG—peptide gels with peptide concentrations of 15 mM had swelling ratios that were significantly higher than those systems with lower concentrations of peptide attached. However, it is important to note that the change in swelling is related to both variations in the gel composition and structure.

3. Conclusions

A thiol—acrylate mixed mode photopolymerization reaction was used to synthesize peptide-functionalized PEG gels. In general, the polymerization proceeded to completion in <10 min using 365 mW UV light at an intensity of $\sim 5 \text{ mW}/\text{cm}^2$. Greater than $\sim 94\%$ of the thiol-presenting peptide sequence in the initial comonomer solution was reacted into the final gel with the exception of a tryptophan-containing system, reaching only 87% peptide incorporation. The efficient incorporation of peptide sequences using this photoinitiated reaction depends on the amino acid sequence, specifically the reactivity of the cysteine group. Hydrogen bonding and positively charged amino acid groups next to the cysteine molecule increase the reactivity of the thiol group, thereby increasing the rate of reaction and

peptide conversion. In contrast, bulky and hydrogen-donating amino acids were seen to decrease the incorporation of peptides into the network, through reduction of the cysteine reactivity. The use of this polymerization scheme to introduce peptides into a PEG network provides an easy, robust, cost-efficient method, which allows a high degree of peptide incorporation (>94%) when the ratio of the acrylate to peptide functionalities is 4. However, one must consider the chemistry of the peptide sequence, especially the sequence adjacent to the cysteine functionality, and its effects on the overall reactivity of the thiol.

4. Materials and Methods

4.1. Synthesis of Poly(ethylene glycol) and Peptide Motifs.

Poly(ethylene glycol) diacrylate (PEGDA) was synthesized by dissolving PEG of weight-average molecular weight 4600 Da in anhydrous dichloromethane under argon for 15 min. Triethylamine (TEA) in a 2:1 molar excess was added to the solution and mixed under argon for 15 min. Acryloyl chloride at a 2.5:1 molar excess, mixed with anhydrous dichloromethane was added dropwise into the PEG/TEA solution, which then reacted overnight under argon. The PEG product was concentrated under reduced pressure and filtered to remove excess salts, precipitated in cold ethyl ether, filtered, and dried in a desiccator overnight. After drying, the PEGDA was redissolved in dH_2O and dialyzed (Spectrum, 1000 MWCO) over 24 h with three dH_2O exchanges. A ^1H NMR analysis of the dialyzed PEGDA product revealed an average of 88% acrylation through comparison of the acrylate hydrogen to ethylene oxide backbone hydrogen integrations.

The peptide sequences CGGGGG (cysteine–glycine–glycine–glycine–glycine–glycine, N-terminus to C-terminus), CDGGGG (cysteine–aspartic acid–glycine–glycine–glycine–glycine, N-terminus to C-terminus), CSGGGG (cysteine–serine–glycine–glycine–glycine–glycine, N-terminus to C-terminus), CRGGGG (cysteine–arginine–glycine–glycine–glycine–glycine, N-terminus to C-terminus), CWGGGG (cysteine–tryptophan–glycine–glycine–glycine–glycine, N-terminus to C-terminus), CGGGGC (cysteine–glycine–glycine–glycine–glycine–cysteine, N-terminus to C-terminus), and CRGDSG (cysteine–arginine–glycine–aspartic acid–serine–glycine, N-terminus to C-terminus) were synthesized using a solid phase peptide synthesizer (Applied Biosystems, model 433A). The peptide sequences were cleaved from the resin and deprotected using trifluoroacetic acid (TFA) (Sigma), phenol, and triisopropylsilane TIPS (Sigma). All peptides were then precipitated in diethyl ether and desiccated for 2 days. The dried product was redissolved in dH_2O and lyophilized. MALDI-TOF spectroscopy was run on the lyophilized product to verify peptide molecular weight and structure. The final product was incorporated into the PEG hydrogel network through a photoinitiated thiol–acrylate reaction with the thiol groups located on the cysteines. In all cases, a solution of 10 wt % diacrylated poly(ethylene glycol) (PEGDA) was dissolved in PBS (neutral pH), and the photoinitiator, 4-(2-hydroxyethoxy)phenyl-(2-hydroxy-2-propyl) ketone (I2959), was added at 0.05 wt %. PEG–peptide systems contained 10 mM peptide, as determined via amine assays to verify concentration of peptide. Each macromer solution was photopolymerized at 365 nm light with an intensity of $\sim 5 \text{ mW/cm}^2$ for 10 min at room temperature. Figure 1 displays the chemical structure of all components used in these studies.

4.2. Determination of Conversion of Functional Groups. FTIR studies were performed on all PEG–peptide systems, including a plain PEG system, used as a control. The samples were polymerized under UV light at for 0, 20, 60, 120, 180, 300, 480, and 600 s. Five 60 μL samples were made at each time point for each sample for a more complete analysis of conversion. The samples made for each condition, at each time point, were lyophilized, ground into a powder, and resuspended in methylene chloride. The resuspended samples were coated onto a CaF_2 crystal and left to air-dry before taking measurements. Near-FTIR was employed to determine the differences, in a sample, between the acrylate peaks at $\sim 1636 \text{ cm}^{-1}$

as normalized to the $\text{C}=\text{O}$ peak at 1713 cm^{-1} for each time point. Conversion was calculated as follows:²⁹

$$X = 1 - \left(\frac{\text{C}=\text{C}_t}{\text{C}=\text{O}_t} \right) \bigg/ \left(\frac{\text{C}=\text{C}_0}{\text{C}=\text{O}_0} \right) \quad (5)$$

The Ellman's assay,³⁰ to measure thiol conversion, was completed in much the same manner as the FTIR studies explained above. Samples were polymerized as described above at the same time points for consistency in data analysis. The samples were lyophilized and resuspended in Ellman's assay buffer, containing 0.1 M sodium phosphate and EDTA. The concentration of thiol groups in a sample were monitored through the colorimetric dye change as read at an Abs of 405 nm. Sample concentrations were determined from a standard curve of known concentrations of L-cysteine. The calculated conversion of the thiol groups was related to the concentration of acrylate functionalities on the PEGDA, which was determined to be 88% acrylated. No difference in hydrogel physical properties was noted to be significant at an acrylation of 88% for these studies.

4.3. Measurement of Peptide Incorporation. The percent peptide incorporation for each peptide sequence was measured via a combination of techniques. Samples were polymerized as described above, and the soluble fraction of the samples was collected. Each soluble fraction was then analyzed via the fluorol-dehyde assay, which measures for free amines. The soluble fraction of each sample was combined with an *o*-phthalaldehyde (OPA) reagent, and the reaction of the reagent with a free primary amine was measured via fluorescence. The amount of free amine measured in the soluble fraction was compared to the initial concentration of free amine prior to polymerization to determine a percent incorporation of peptide. These values were compared to the conversion of thiol groups as determined from the Ellman's assay as described above to ensure that the amount converted was similar to that actually incorporated.

4.4. Determination of pK_a of Cysteine. The pK_a of cysteine was monitored via a change in the thiolate anion absorbance at 233 nm as described previously.¹⁸ The peptides used in this study, unreacted with the PEG monomer, were dissolved at a concentration of 0.1 mM, in a buffer system composed of 0.1 M NaCl and 0.01 M sodium phosphate. The pH of the system was altered using strong 4 N HCl and/or 4 N NaOH. A set of three absorbance measurements for each peptide were taken at pH levels of 6.1, 6.8, 7.4, 8, 8.6, 9, 10, 12, and 14.

4.5. Rheological Characterization of Gelation and the Elastic Modulus. The gelation and final gel properties of PEG–peptide systems were measured via small-amplitude oscillatory shear testing on an Ares 4400 rheometer (TA Instruments). PEG–peptide solutions were prepared and placed on a Peltier plate, or temperature controller, for the rheometer. The monomer solution was then pressed between a quartz crystal to allow for reflectance of UV light into the sample, while the Peltier plate held a gap width of 200 μm . A Novacure mercury arc lamp was used to supply $\sim 7 \text{ mW/cm}^2$ light to the sample focused around the 365 nm wavelength using a 320–500 nm band-pass filter. Data were collected using parallel plate geometry with a diameter of 20 mm. The system was coated with a thin layer of polydimethylsiloxane to avoid evaporation during testing. The solution was held at 25 $^\circ\text{C}$ for each of the experiments performed. Each of the samples measured was investigated at a frequency of 10 Hz and a strain of 50%. Strain sweeps were run on all of the samples to determine whether measurements were consistently collected in the linear regime. The cross-linking density for each PEG–peptide system was calculated based upon the elastic modulus (G') and the equilibrium swelling ratio (Q) in reference to the amount of water put into each sample during modulus measurements. Therefore, Q for each PEG–peptide sample was equivalent in the rheological measurements and cross-linking density calculations.

4.6. Equilibrium Swelling Measurements. PEG–peptide and a plain PEG gel disks (5 mm \times 1 mm) were created at an n of 5, for each condition, and allowed to swell in dH_2O for 3 days. The

wet weight of each sample was measured prior to placing each of the samples in a vacuum oven at 60 °C for 3 days. Afterward, the samples were weighed to determine their dry weight and a mass swelling ratio (q) was calculated as the ratio of wet weight to dry weight. An equilibrium swelling ratio (Q) was determined from the mass swelling ratio (q) and the corresponding densities of the polymer and the swelling solution.

4.7. Statistics. Data are presented as mean \pm standard deviation of the replicates. A Student's t test was utilized to compare data sets, with p values less than 0.05 signifying significant differences.

Acknowledgment. Funding for this project was provided by National Institutes of Health (DE12998) as well as a grant from the Graduate Assistantship in Areas of National Need fellowship to C.N.S.

References and Notes

- (1) Nuttelman, C. R.; Tripodi, M. C.; Anseth, K. S. Synthetic hydrogel niches that promote hMSC viability. *Matrix Biol.* **2005**, *24*, 208–218.
- (2) Salinas, C. N.; Cole, B. B.; Kasko, A. M.; Anseth, K. S. Chondrogenic differentiation potential of human mesenchymal stem cells photoencapsulated within poly(ethylene glycol)-arginine-glycine-aspartic acid-serine thiol-methacrylate mixed-mode networks. *Tissue Eng.* **2007**, *13*, 1025–34.
- (3) West, J. L. H., J. A. *Bioactive Polymers*; Altala, A. M., D. J., Langer, R., Vacanti, J. P., Eds.; Birkhauser: Boston, 1997.
- (4) Mann, B. K.; Gobin, A. S.; Tsai, A. T.; Schmedlen, R. H.; West, J. L. Smooth muscle cell growth in photopolymerized hydrogels with cell adhesive and proteolytically degradable domains: synthetic ECM analogs for tissue engineering. *Biomaterials* **2001**, *22*, 3045–5.
- (5) Rowley, J. A.; Madlambayan, G.; Mooney, D. J. Alginate hydrogels as synthetic extracellular matrix materials. *Biomaterials* **1999**, *20*, 45–53.
- (6) Barry, F.; Boynton, R.; Liu, B.; Murphy, J. Chondrogenic differentiation of mesenchymal stem cells from bone marrow: Differentiation-dependent gene expression of matrix components. *Exp. Cell Res.* **2001**, *268*, 189–200.
- (7) Belcheva, N.; Baldwin, S. P.; Saltzman, W. M. Synthesis and characterization of polymer-(multi)-peptide conjugates for control of specific cell aggregation. *J. Biomater. Sci., Polym. Ed.* **1998**, *9*, 207–26.
- (8) Carr, P. W.; Bowers, L. D. *Immobilized Enzymes in Analytical and Clinical Chemistry*; John Wiley: New York, 1980.
- (9) Lutolf, M. P. H., J. A. Synthesis and Physicochemical Characterization of End-Linked Poly(ethylene glycol)-co-peptide Hydrogels Formed by Michael-Type Addition. *Biomacromolecules* **2003**, *4*, 713–722.
- (10) Mann, B. K.; Tsai, A. T.; Scott-Burden, T.; West, J. L. Modification of surfaces with cell adhesion peptides alters extracellular matrix deposition. *Biomaterials* **1999**, *20*, 2281–6.
- (11) Jemal, M.; Hawthorne, D. J. Quantitative determination of BMS-186716, a thiol compound, in rat plasma by high-performance liquid chromatography-positive ion electrospray mass spectrometry after hydrolysis of the methyl acrylate adduct by the native esterases. *J. Chromatogr. B: Biomed. Sci. Appl.* **1997**, *698*, 123–32.
- (12) Schelte, P.; Boeckler, C.; Frisch, B.; Schuber, F. Differential reactivity of maleimide and bromoacetyl functions with thiols: application to the preparation of liposomal diepitope constructs. *Bioconjugate Chem.* **2000**, *11*, 118–23.
- (13) Romanowska, A.; Meunier, S. J.; Tropper, F. D.; Laferriere, C. A.; Roy, R. Michael additions for syntheses of neoglycoproteins. *Methods Enzymol.* **1994**, *242*, 90–101.
- (14) Masri, M. S.; Friedman, M. Protein reactions with methyl and ethyl vinyl sulfones. *J. Protein Chem.* **1988**, *7*, 49–54.
- (15) Lecamp, L. H. F.; Youssef, B.; Bunel, C. Photoinitiated cross-linking of a thiol-methacrylate system. *Polymer* **2001**, *42*, 2727–2736.
- (16) Cramer, N. B. B.; Christopher, N. Kinetics of thiol-ene and thiol-acrylate photopolymerizations with real-time fourier transform infrared. *J. Polym. Sci., Part A* **2001**, *39*, 3311–3319.
- (17) Cramer, N. B. R.; Sirish, K.; O'Brien, A. K.; Bowman, C. N. Thiol-Ene Photopolymerization Mechanism and Rate Limiting Step Changes for Various Vinyl Functional Group Chemistries. *Macromolecules* **2003**, *36*, 7964–7969.
- (18) Lutolf, M. P.; Tirelli, N.; Cerritelli, S.; Cavalli, L.; Hubbell, J. A. Systematic modulation of Michael-type reactivity of thiols through the use of charged amino acids. *Bioconjugate Chem.* **2001**, *12*, 1051–6.
- (19) Temenoff, J. S.; et al. Thermally cross-linked oligo(poly(ethylene glycol) fumarate) hydrogels support osteogenic differentiation of encapsulated marrow stromal cells in vitro. *Biomacromolecules* **2004**, *5*, 5–10.
- (20) Elbert, D. L.; Hubbell, J. A. Conjugate addition reactions combined with free-radical cross-linking for the design of materials for tissue engineering. *Biomacromolecules* **2001**, *2*, 430–41.
- (21) West, J. L. H., J. A. Polymeric biomaterials with degradation sites for proteases involved in cell migration. *Macromolecules* **1999**, *32*, 241–244.
- (22) Reddy, S. K.; Okay, O.; Bowman, C. N. Network Development in Mixed Step-Chain Growth Thiol-Vinyl Photopolymerizations. *Macromolecules* **2006**, *39*, 8832–8843.
- (23) Rydholm, A. E. B.; Christopher, N.; Anseth, K. S. Degradable thiol-acrylate photopolymers: polymerization and degradation behavior of an in situ forming biomaterial. *Biomaterials* **2005**, *26*, 4495–4506.
- (24) Shaked, Z.; Szajewski, R. P.; Whitesides, G. M. Rates of thiol-disulfide interchange reactions involving proteins and kinetic measurements of thiol pKa values. *Biochemistry* **1980**, *19*, 4156–66.
- (25) Winter, H. H. Can the Gel Point of a Cross-linking Polymer Be Detected by the G' - G'' Crossover? *Polym. Eng. Sci.* **1987**, *27*, 1698–1702.
- (26) Nielson, L. E. *Mechanical Properties of Polymers*; Van Nostrand Reinhold: New York, 1962.
- (27) Young, R. J.; Lovell, P. A. *Introduction to Polymers*; CRC Press: Boca Raton, FL, 1991.
- (28) Bryant, S. J.; Anseth, K. A. In *Scaffolding in Tissue Engineering*; Marcel Dekker: New York, 2005; p 638.
- (29) Biswal, D.; Hilt, J. Z. Microscale analysis of patterning reactions via FTIR imaging: Application to intelligent hydrogel systems. *Polymer* **2006**, *47*, 7355–7360.
- (30) Ellman, G. L. Tissue sulfhydryl groups. *Arch. Biochem. Biophys.* **1959**, *82*, 70–7.
- (31) Canal, T.; Peppas, N. A. Correlation between mesh size and equilibrium degree of swelling of polymeric networks. *J. Biomed. Mater. Res.* **1989**, *23*, 1183–93.

MA800621H